



HHS Public Access

Author manuscript

J Mol Biol. Author manuscript; available in PMC 2017 May 08.

Author Manuscript

Author Manuscript

Author Manuscript

Author Manuscript

Published in final edited form as:

J Mol Biol. 2016 May 8; 428(9 Pt B): 1833–1845. doi:10.1016/j.jmb.2016.03.016.

Structural dynamics and mechanochemical coupling in DNA gyrase

Aakash Basu¹, Angelica C. Parente^{2,3}, and Zev Bryant^{3,4,*}

¹Department of Physics, University of Illinois at Urbana-Champaign, Urbana, IL 61801, USA

²Program in Biophysics, Stanford University, Stanford, CA 94305, USA

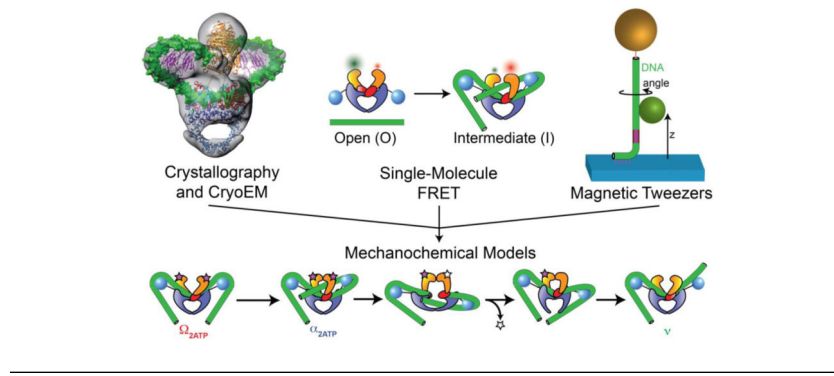
³Department of Bioengineering, Stanford University, Stanford, CA 94305, USA

⁴Department of Structural Biology, Stanford University Medical Center, Stanford, CA 94305, USA

Abstract

Gyrase is a molecular motor that harnesses the free energy of ATP hydrolysis to perform mechanical work on DNA. The enzyme specifically introduces negative supercoiling in a process that must coordinate fuel consumption with DNA cleavage and religation and with numerous conformational changes in both the protein and DNA components of a large nucleoprotein complex. Here we present a current understanding of mechanochemical coupling in this essential molecular machine, with a focus on recent diverse biophysical approaches that have revealed details of molecular architectures, new conformational intermediates, structural transitions modulated by ATP binding, and the influence of mechanics on motor function. Recent single-molecule assays have also illuminated the reciprocal relationships between supercoiling and transcription, an illustration of mechanical interactions between gyrase and other molecular machines at the heart of chromosomal biology.

Graphical Abstract



* Author for correspondence: zevry@stanford.edu.

Publisher's Disclaimer: This is a PDF file of an unedited manuscript that has been accepted for publication. As a service to our customers we are providing this early version of the manuscript. The manuscript will undergo copyediting, typesetting, and review of the resulting proof before it is published in its final citable form. Please note that during the production process errors may be discovered which could affect the content, and all legal disclaimers that apply to the journal pertain.

DNA gyrase remodels the bacterial chromosome by introducing negative supercoils, playing an essential role in compacting the genome and solving topological challenges associated with replication and transcription [1]. The enzyme forms a dynamic complex with >100 bp of DNA, and must form and break protein-DNA interactions and rearrange the sharply bent DNA path during each ATP-fueled conformational cycle. As has been extensively reviewed elsewhere [2, 3], many structural and biochemical features of the gyrase mechanism have been identified over the past several decades since the discovery of the enzyme. However, a concrete understanding of the structure and dynamics of the complete holoenzyme complex has been elusive because of the size of the machine, the extent of its interactions with the DNA substrate, and the number of moving parts. Over the past five years, biophysical measurements have provided new insight into conformational states and kinetic pathways that underlie the mechanochemical function of the gyrase motor. We discuss these recent results, related experiments, and remaining questions after briefly introducing some biochemical and structural background.

DNA gyrase is a specialized type II topoisomerase

Gyrase is an A_2B_2 tetramer (Fig 1a) that shares a core set of domains and a duplex strand passage mechanism with other members of the type IIA topoisomerase family [3]. In this family, three protein-protein interfaces form gates that can open and close to allow passage of DNA through the enzyme. The segment of duplex DNA destined to be cleaved, called the G- (or Gate-) segment, binds at the central DNA gate formed by the Topoisomerase-Primase (TOPRIM) domain together with the Winged Helix Domain (WHD) containing the active site tyrosine that forms a transient 5'-phosphotyrosyl protein-DNA linkage in the cleaved state. DNA-bound structures of the binding and cleavage core for gyrase and other type IIA topoisomerases show a dramatic bend in the G-segment [4, 5]. A second DNA segment known as the T- (or transfer) segment enters through the N-gate, in an upper cavity formed by GHKL ATPase domains that can dimerize upon ATP binding and may communicate the nucleotide state to the DNA gate via conformational changes involving the intervening transducer domain [6, 7]. After passing through the transiently cleaved G-segment and opened DNA gate into a lower cavity framed by coiled-coil domains, the T-segment can exit through a final reversible interface known as the C-gate. In a closed circular molecule, the overall reaction inverts a node between the T- and G-segments and therefore changes the linking number of the DNA in a step of 2 [8].

The globular C-terminal domain (CTD) of DNA gyrase (Fig. 1a) diverges from other type IIA topoisomerases [9] and is essential for the unique ability of DNA gyrase to introduce, rather than merely relax, supercoils (Fig. 1b). The directionality of supercoiling can be enforced by chirally wrapping DNA between the G-segment and the T-segment, trapping (+) writhe and presenting a (+) node whose inversion changes the linking number by -2 [8, 10]. Gyrase wraps DNA as probed by exonuclease, DNAase I, and hydroxyl radical footprinting experiments [11–13], and constrains (+) writhe in the absence of nucleotide as shown by topoisomer footprinting [10] [14]. The CTD is essential for these properties and for directional supercoiling; its deletion converts gyrase into a conventional type II topoisomerase [15, 16]. Structural and functional studies of the isolated CTD [17] [18]

showed that it has a beta-pinwheel fold with a basic patch around the outer edge, and can bind and bend DNA.

Structural investigations of global architecture

As of this writing, there is no reported high-resolution structure of full-length gyrase in complex with DNA. The arrangement of the CTDs relative to the core and the path of the DNA around the CTDs have been the subject of study and debate. A crystal structure of the related topoisomerase IV [9] showed the CTDs in plane with the DNA gate, and small angle X-ray scattering models have shown the CTDs in a lower position near the exit gate in GyrA [19] and the holoenzyme [20], leading to proposals in which the CTDs are mobile during the conformational cycle [19]. An important goal for describing the DNA gyrase mechanism is to define conformations of the overall holoenzyme and the associated DNA visited during the mechanochemical cycle, and characterize transitions in this global architecture dependent on substeps in fuel consumption.

A recent cryoelectron microscopy study [21] provides the most complete picture to date of the architecture of full-length DNA gyrase, and the first direct visualization of DNA wrapped around the CTDs (Fig. 2a). A 23 Å map of the *T. thermophilus* gyrase holoenzyme was obtained in complex with 155 bp DNA, stabilized with ciprofloxacin and AMPPNP. The N-gate is closed and the CTDs are in plane with the DNA gate, with clear density attributable to DNA bent around them. The conformation was proposed to represent a state that traps a T-segment prior to strand passage, although the included DNA appears to be of insufficient length to present a T-segment in the complex that was obtained. The modeled DNA (Fig. 2a) includes a shallower G-segment bend than has been seen in crystal structures of various type IIA topoisomerases in complex with DNA (Fig. 2b), including structures of the gyrase cleavage core bound to shorter DNA fragments [4, 5], suggesting an influence of the CTDs on the central DNA conformation. The authors also obtained a 17 Å reconstruction of the holoenzyme in the absence of DNA, in which the CTDs are not visible due to conformational heterogeneity. For both reconstructions, the closed N-gate is seen in a “domain swapped” configuration previously observed [22] in a recent structure of the full length *S. cerevisiae* topoisomerase II in complex with G-segment DNA and AMPPNP (Fig. 2b), which was proposed to represent a post-strand passage conformation that prevents regression of the T-segment back up through the DNA gate.

Unlike crystallography and cryoelectron microscopy, single-molecule measurements are able to probe only limited structural degrees of freedom. These methods are nevertheless powerful tools for characterizing dynamic molecular machines because they can be used on heterogeneous populations in solution, report on conformational distributions, directly follow the dynamics of actively cycling enzymes, and apply controlled mechanical perturbations. Three major single-molecule approaches have been applied to DNA gyrase, each exploiting one or more of the attributes above: (1) FRET measurements have been used to characterize conformational distributions under varying conditions relevant to the mechanochemical cycle, notably contributing to our understanding of how protein domains rearrange in response to DNA and nucleotide binding; (2) a specialized magnetic tweezers technique known as rotor bead tracking (RBT) [23] has been used to directly follow the dynamics of

supercoiling and nucleotide-dependent transitions between states that differ in their DNA conformation; and (3) “conventional” magnetic tweezers assays [24] have been used to probe the effects of force, torque, and DNA mechanics on the gyrase molecular motor.

FRET measurements of conformational states

Single-molecule fluorescence resonance energy transfer (smFRET) can provide a measurement of the distance between two dyes attached at known positions to a molecule of interest. Gyrase conformations have been extensively studied [25–31] using an smFRET experimental design in which molecules are observed when they diffuse through a confocal volume [32], producing a brief burst of fluorescence (Fig. 3). This smFRET approach allows distributions of FRET values to be recorded over many molecules while avoiding the complications of surface interactions. The goal of the assay is principally to capture snapshots rather than dynamics, since the observation time for each molecule is short in comparison with the timescale of the mechanochemical cycle. This may be contrasted with the longer observation times enabled by a common alternative approach [33] in which molecules are affixed to a coverslip and typically illuminated using total internal reflection (TIRF).

smFRET measurements on *B. subtilis* gyrase have shown how both the N-gate conformation and the CTD position depend on the nucleotide and the DNA. These studies have revealed unanticipated conformational states, and have provided snapshots that are suggestive of a series of conformational changes leading to directional strand passage. To monitor the N-gate, Gubaev *et al* [27] produced gyrBgyrA fusion proteins labeled at each of several alternative positions on the ATPase domain, and measured FRET between equivalent positions on symmetric dimers (Fig. 3b). As expected, FRET values are consistent with an open N-gate in the apo state, shifting to a closed state in presence of AMPPNP (Fig. 3c). Unexpectedly, the authors discovered an intermediate (narrowed) conformation of the N-gate that is populated when DNA is bound even in the absence of nucleotide (Fig. 3d). Formation of the intermediate state requires >110bp of DNA, suggesting that the narrowed gate depends on DNA wrapping around the CTDs. A chiral wrapping model for this state is supported by the observation of a reduced population of the intermediate state in the presence of negative DNA supercoiling, which is expected to oppose positive superhelical wrapping. The results were interpreted to suggest an ordered progression that coordinates DNA wrapping with N-gate closure, in which the N-gate partially closes when the chiral wrap is formed, then closes completely upon ATP binding to trap a T-segment poised for strand passage (Fig. 3e).

For directly measuring CTD movements, heterodimeric gyrA mutants were purified to enable intramolecular labeling with a donor/acceptor dye pair on the CTD and body of a single gyrA subunit [30]. By measuring differences in FRET distributions when exposed to gyrB and different lengths of DNA, the authors found that the CTDs are positioned toward the exit gate in the gyrA dimer, move slightly further away from the body in the gyrA:gyrB holoenzyme, and move upward when DNA is bound (Fig. 3f). The inferred change in CTD position between the gyrA dimer and the DNA-bound holoenzyme is qualitatively similar to a comparison between the earlier SAXS structure for gyrA [19] and the *T. thermophilus*

cryoEM structure that appeared after these FRET studies [34]; the results with DNA contrast with the SAXS model obtained for the *E. coli* holoenzyme [20]. smFRET histograms for some CTD-body labeling locations were bimodal, suggesting there may be either structural asymmetry between the two CTDs or heterogeneity of a single CTD position. Repositioning the CTDs requires neither nucleotide, nor cleavage, nor a long enough DNA template to present a T-segment, suggesting an ordered progression in which CTD movement is an early step in the catalytic cycle, positioning the CTD for chiral wrapping to present a T-segment in the narrowed N-gate followed by N-gate closure.

Solution confocal smFRET measurements can provide richly detailed information about conformations accessible to DNA gyrase. The use of multiple FRET pair positions places constraints on the 3D architectures of complexes that have resisted conventional structural characterization, and exhaustive sampling of conditions has helped determine coupling between protein conformations and chemical states relevant to the mechanochemical cycle of the enzyme. However, because the assay does not provide either dynamic tracking of conformations over the timescale of the cycle or a readout of progress of the supercoiling reaction, the temporal ordering, kinetics, and functional context of conformational states cannot be directly determined. Rotor bead tracking (RBT), which measures real-time changes in the extension and linking number of a single tethered DNA molecule [23], is a complementary technique that has been exploited to directly monitor the mechanical output of the gyrase supercoiling reaction while tracking rearrangements of the nucleoprotein complex manifested as dynamic changes in the conformation of the DNA (Fig. 4).

RBT measurements of nucleoprotein dynamics

RBT relies on measuring the angular position of a submicron bead (the “rotor”) attached to the side of a single stretched DNA molecule (Fig. 4a). In assays of DNA gyrase, the introduction of two negative supercoils causes the rotor to spin by two full rotations per enzymatic cycle, while a distal swivel prevents the permanent accumulation of torsional strain. Structural intermediates within the cycle appear as angular dwells that can be placed along the natural repeating two-rotation reaction coordinate. Initial RBT measurements of DNA gyrase showed processive bursts in strict multiples of two rotations (similar to Fig. 4b, above) as expected [35], and found that the rate-limiting angular dwell occurs at the ~0 (even) rotation mark, implying that the enzyme predominantly waits in a state that does not trap any writhe. This state was initially assumed to have released the wrapped DNA, but later RBT measurements [36] — which included tracking of the rotor height (z) as a direct measure of DNA sequestration (Fig. 4b, below) for the first time — showed that although no writhe is trapped, the enzyme in fact sequesters >100 bp of DNA in this unanticipated nucleoprotein conformation now dubbed the Ω state.

The properties of the Ω state are explained by a schematic model in which the DNA flanking the G-segment is bent around the CTDs without forming a chiral wrap [36]. A major remodeling transition is required in order to reach a chirally wrapped configuration, now dubbed the α state. Both of these structural intermediates may be observed in RBT experiments and visualized as populations in two dimensional histograms of (angle, z) coordinates visited during active supercoiling (Fig. 4c). The Ω -to- α transition, which

Author Manuscript

Author Manuscript

Author Manuscript

Author Manuscript

dominates the kinetics of supercoiling, was proposed to involve CTD motion and correspond to T-segment capture. ATP dramatically accelerates the rate of this remodeling transition, revealing a new role for nucleotide binding in promoting the formation of the chiral wrap. Quantitative analysis of [ATP]-dependent substep kinetics [36] led to a branched kinetic model for early events in the gyrase cycle (Fig. 4e): the central Ω -to- α remodeling transition can occur slowly via thermal sampling in the absence of ATP, or quickly when 2 ATP molecules are bound. The α state is chirally wrapped and contains a poised T-segment; it requires 2 bound ATP molecules to progress forward via strand transfer, and can otherwise thermally revert to the Ω state. Notably, thermal interconversion of Ω and α quantitatively explains bulk topoisomer footprinting assays, in which ~0.8 positive supercoils were found to be trapped per gyrase enzyme in the absence of nucleotide [10, 14]. RBT, a single-molecule analog of topoisomer footprinting, recapitulates a similar value as an average over three dynamically exchanging conformations: the Ω state, which traps ~0 supercoils, and two isoforms of the α state in which either ~1 or ~1.7 supercoils are trapped. This result illustrates the power of single-molecule measurements to resolve heterogeneous populations [36], which should be considered when interpreting other bulk measurements of the complex such as DNA protection studies [11–13] that may similarly reflect averages over conformational ensembles.

RBT provides an incomplete picture of nucleoprotein dynamics because of limited degrees of freedom (only the angle and extension of the DNA are monitored) and also because of finite spatiotemporal resolution: Brownian noise of the rotor obscures the detection of short-lived states or small conformational changes [23]. An important advance in RBT technology was therefore the introduction of AuRBT, which uses evanescent darkfield imaging to track gold nanoparticles employed as high-speed probes of DNA angle and extension [37], offering dramatic improvements over previous RBT methods. In an initial application of AuRBT to DNA gyrase (Fig. 4d), not only are individual steps between dominant dwells in the Ω state very clearly visualized even at saturating [ATP], but a new transient state between these dwells can also be seen for the first time [37]. In this “ ν state”, substantial DNA contour length is released from the enzyme, leading to a model in which DNA is briefly released from one or both CTDs after strand passage, and then recaptured to begin the next cycle. In the picture that emerges from RBT and AuRBT measurements (Fig. 4e), the formation of the chiral wrap during each cycle is a multistep process: beginning from the ν state, DNA is first quickly bent around the CTDs to form the Ω state, then goes through a slower rearrangement relying on CTD motion to reach the chirally wrapped α state.

While RBT measurements have illuminated major global remodeling transitions in the gyrase:DNA complex, more work is needed to establish the molecular details of these structural transitions. The DNA path for each state has only been depicted in schematic cartoons; RBT measurements are insufficient to precisely define this path, and states may also contain variable structures, substates, and unresolved intermediates that contribute to the spread observed in angle and z values (Fig. 4c). The model for the DNA path presented in the recent cryoEM study resembles cartoons of the ~1.7 supercoil-trapping isoform of the α state, but should be interpreted with caution since (1) there is no direct visualization of a trapped T-segment; (2) the complex is stabilized using a nucleotide and drug combination in a state with an unknown relationship to the functional conformational cycle; and (3) the *T*.

thermophilus enzyme used for cryoEM may have distinct properties from the distantly related *E. coli* enzyme used in RBT measurements.

Common themes and outstanding questions from single-molecule dynamics

Descriptions of gyrase structural dynamics inferred from smFRET and RBT studies have some similar features, including mobile CTDs, ordered progressions of conformational intermediates leading to chiral wrapping and T-segment capture, and coupling between the conformations of the DNA and the N-gate. However, it is unclear that any one-to-one mapping can be made between protein conformational states identified using FRET and DNA conformational states identified using RBT. It was suggested [36] that the ATP-free chirally wrapped α state contains a narrowed N-gate, which might partially trap a T-segment and help explain long dwells in this state in RBT experiments as well as stabilization of the narrowed N-gate by conditions favoring chiral wrapping in FRET experiments [27]. In this model, the narrowed N-gate favors productive strand passage by creating a binding site to retain the T-segment awaiting complete N-gate closure and strand passage.

The Ω conformation has also been proposed to inhibit N-gate closing [36], helping gyrase avoid futile cycles of ATP hydrolysis before a T-segment is bound. In this model, the closed N-gate occurs only transiently during active supercoiling, which agrees with smFRET measurements using hydrolysable ATP [27]. The Ω conformation has been also been depicted with upwardly positioned CTDs [36], but definitive determination of the correspondence between DNA and protein conformations awaits experiments that measure these degrees of freedom simultaneously, as might be accomplished using a multimodal single-molecule approach [38–40] such a proposed combination of AuRBT with FRET [37].

Comparisons between the confocal smFRET and RBT measurements are further complicated by the use in these two experiments of gyrase from two divergent species (*B. subtilis* and *E. coli*, respectively), which may have differences in the proportion of the cycle spent in different substates, or possibly more dramatic mechanistic differences. Significant differences are hinted at by the apparent failure of *B. subtilis* gyrase to perform a single round of strand passage supported by AMPPNP, in contrast to *E. coli* [31, 41] and by differing functional requirements for the C-terminal tail of the CTD, which has been implicated as a physical element responsible for coordination between chiral wrapping and the ATPase cycle in both species and is absolutely required for supercoiling in *E. coli* [42] but not in *B. subtilis* [29]. Direct comparisons between the two species in identical single-molecule assays will be important for distinguishing general from specific features of the gyrase mechanochemical cycle.

A strength of the RBT studies is that they provide kinetic as well as structural information, yielding a quantitative dynamic description of the motor cycle in which structural transitions are coupled to specific substeps in fuel consumption. However, work to date has left this mechanochemical description of the motor mechanism substantially incomplete: the ν state has not been characterized in enough detail to either define its geometry or determine whether its dynamics depend on the nucleotide cycle, and global conformational changes

coupled to hydrolysis and product release have not been directly probed. Future RBT experiments conducted with varying nucleotides, including non-hydrolysable analogs, may address these questions and provide further valuable points of comparison with bulk solution measurements. Hydrolysis has previously been studied using bulk single-turnover kinetics in the related enzyme yeast topoisomerase II, and it was found that ATP hydrolysis dramatically accelerates strand passage [43], although it has long been known that hydrolysis is not strictly required for this step [44]. If this turns out to be true for gyrase as well, it will complete a repeating pattern of loosely coupled structural transitions, in which the Ω -to- α chiral wrapping transition can happen slowly without ATP or quickly when ATP is bound, presenting a T-segment that can then be transferred slowly with ATP binding alone or quickly when ATP is hydrolyzed. Chemical substeps thus modulate the conformational energy landscape to guide the motor toward productive forward progress, without requiring a one-to-one correspondence between chemical and conformational states.

Mechanics of gyrase and its interactions in the chromosome

Mechanical perturbations applied in single-molecule experiments are valuable for probing the energy landscapes of molecular motors [45] and for testing responses to stresses that may be experienced in cells. The first RBT measurements of DNA gyrase [35] found that the processivity of the motor is exquisitely sensitive to tension in the DNA molecule, while the supercoiling velocity of the motor is relatively insensitive to this parameter. In light of subsequent work [36], this behavior may be understood since dissociation involves a large change in DNA extension when the enzyme releases sequestered contour length, while the rate-limiting step in the supercoiling cycle involves a transition between two states (Ω and α) that both sequester extensive contour length and thus have similar extensions. Transitions to and from the transient ν state [37] are expected to be highly tension-sensitive due to the large changes in extension relative to Ω and α , but this perturbation has not been characterized directly and would not be expected to affect the supercoiling velocity under moderate tensions. The major influence of even sub-pN forces on processivity, and potentially on the dynamics of transient states, could be a control mechanism *in vivo* and should also be accounted for when comparing single-molecule measurements under tension to bulk solution measurements.

Torque may be a more important parameter than tension in cellular contexts, where the enzyme must work against accumulated negative supercoiling or may act on transiently positively supercoiled domains. In the RBT assays used for gyrase, supercoils do not accumulate, but alternative assays have been used to probe this condition. Nollmann *et al* measured gyrase activity on both positively and negatively supercoiled DNA molecules [46], using a magnetic tweezers assay in which changes in linking number are reflected in changes in DNA extension due to the accumulation of plectonemic structures. They noted robust relaxation of positive supercoils even under elevated tensions, and also observed mechanically induced switching between introduction and relaxation of negative supercoils. Similar results were obtained by Fernandez-Sierra *et al* [47], who also studied the activity of gyrase on diaminopurine-substituted tethers, which have a higher bending stiffness than unsubstituted DNA. *E. coli* gyrase essentially fails to supercoil diaminopurine-substituted DNA, which was ascribed to the additional energy required to achieve the very tightly bent

conformations seen in both the Ω and α states. Sequence-dependent modulation of DNA bending stiffness was proposed as a potential mechanism of localized biological control over gyrase activity [47].

The mechanics of DNA gyrase must be understood in a larger context: gyrase communicates with other cellular machinery through torsional strain in the DNA. It has long been appreciated that torsion generated by gyrase is used to transmit information through the genome and exert sophisticated control over biological processes such as replication initiation and transcription of specific genes, including homeostatic control of gyrase itself [48] and transcriptional responses to metabolic changes that may be sensed directly by the DNA gyrase motor via the cellular ATP energy stores [49, 50]. In a recent striking example [51], oscillating DNA supercoiling levels act as a global regulator of shifting transcriptional programs during the circadian rhythms of cyanobacteria: distinct promoters are simultaneously up- and down-regulated by torsional changes, and inhibition of DNA gyrase is sufficient to induce a transcriptional response that mimics a change in the time of day. Recent single-molecule investigations have investigated the transcriptional side of this mechanical interaction, by measuring how RNA polymerase generates and responds to torque, and by directly observing the impact of gyrase on transcription.

In seminal work, Liu and Wang noted that progression of an elongating transcription complex can generate positive supercoils ahead of and negative supercoils behind the polymerase [52] due to helical tracking on a constrained DNA duplex. This phenomenon may be expected to occur in anchored ~ 10 kb supercoiling domains [53] in the bacterial chromosome (Fig. 5a). To directly measure the effect of accumulated torque on transcription elongation, Ma *et al* used an angular optical trap (Fig. 5b) to follow transcription against a torsional load. Among their observations, they found that RNAP generates positive supercoiling until it stalls at a characteristic torque of ~ 10 pNm. In this experiment, negative supercoils do not accumulate behind the polymerase due to the presence of a free end. In a bacterial cell, positive and negative supercoiling domains generated by transcription may be relaxed by gyrase and topoisomerase I, respectively, and a local imbalance between these topoisomerases could lead to net supercoiling within a chromosomal loop. This scenario was directly investigated [54] using a single-molecule assay for transcription in which the growing nascent RNA produces an increasing fluorescence signal due to binding of a dye (Fig. 5c). With this assay, Chong *et al* were able to measure transcriptional activity on tethered DNA circles that mimic chromosomal loops, and observe the effect of including topoisomerase I and gyrase in the system.

Results on the mechanical interplay of gyrase, topoisomerase I, and RNA polymerase supported the feasibility of a model that may explain the phenomenon of transcriptional bursting in *E. coli* [54]. In this model, excess topoisomerase I continually relaxes negative supercoils generated behind transcribing complexes, while the positive supercoils generated ahead of RNA polymerase are only relaxed when gyrase is present in the supercoiling domain (Fig. 5d). Noting that the number of gyrase holoenzymes in the cell [55] is of the same order as the number of constrained supercoiling domains [53], the model predicts that transcription within a ~ 10 kb domain will switch bimodally between (i) active gene expression when gyrase is present, and (ii) arrest when gyrase is absent and positive

supercoils accumulate to inhibit transcription. This study presents an example of a complex emergent phenomenon that arises from simple interactions between molecular machines in the chromosome, and hints at parallels with the cytoskeletal motor field, where theoretical and experimental studies have shown how collections of motors and filaments may display emergent behaviors dependent on microscopic properties of individual motors such as force-velocity relationships and force-dependent off rates [56].

In order to further relate biophysical measurements to *in vivo* functions, it will be critical to measure varied properties of gyrases found in different organisms, where they may be adapted for a range of cellular requirements. For example, *M. tuberculosis* gyrase, which lacks the C-terminal tail required for coordination of chiral wrapping and ATP binding in *E. coli* [42], acts slowly and stalls at much lower supercoiling densities than the *E. coli* enzyme [57]. Even closely related bacterial species can have differing supercoiling requirements: *Salmonella enterica* serovar Typhimurium supercoils its genome to a lower density than *E. coli* [58]. Few single-molecule measurements have been repeated on more than one species — a comparison between *E. coli* and *Salmonella* reported by Fernandez-Sierra *et al* is a rare exception [47] — and measurements that control for species differences are needed for making consistent biophysical models that integrate data from structural, biochemical, fluorescence, and mechanical experiments. As we have noted, the cryoEM, smFRET, and RBT experiments reviewed here were performed using gyrase from three divergent organisms (*T. thermophilus*, *B. subtilis*, and *E. coli*, respectively), complicating comparisons.

An additional source of varied gyrase behavior is the DNA binding site. Biophysical measurements have exploited sequences that form unusually tight complexes with DNA gyrase. RBT measurements, for example, have made use of a variant of the strong gyrase site from Mu phage [59], in order to increase the processivity of the enzyme [60] and counteract the destabilizing effect of tension. Comparative measurements on diverse sequences, including gyrase binding sites of biological interest such as REP sequences identified in the *E. coli* chromosome [61, 62], will be valuable for generalizing results and relating mechanochemistry to biology.

Toward a mechanochemical description of gyrase motor function

Recent biophysical studies have built upon decades of biochemical and structural investigations to show how coordinated conformational changes in the gyrase nucleoprotein complex lead to motor function. Single-molecule measurements have begun to reveal the complexity of a branched kinetic pathway in which structural transitions are loosely coupled to chemical substeps, and more work is needed to fully define the mechanochemical cycle. Models that relate protein conformational changes to the dynamics of DNA geometry must be tested, and a major challenge for structural biology is to establish the detailed three-dimensional architectures of conformational states identified in single-molecule studies, including the Ω , α , and ν states. Finally, the mechanical capabilities and responses of gyrase and other DNA-associated machines must be understood and may be tested in combinations [54] in order to build a quantitative understanding of an emerging mechanobiology of the chromosome.

Acknowledgments

This work was supported by NIH grants GM106159 and 5U19AI10966202.

References

1. Wang JC. Cellular roles of DNA topoisomerases: a molecular perspective. *Nat Rev Mol Cell Biol*. 2002; 3:430–440. [PubMed: 12042765]
2. Nollmann M, Crisina NJ, Arimondo PB. Thirty years of *Escherichia coli* DNA gyrase: from *in vivo* function to single-molecule mechanism. *Biochimie*. 2007; 89:490–499. [PubMed: 17397985]
3. Schoeffler AJ, Berger JM. DNA topoisomerases: harnessing and constraining energy to govern chromosome topology. *Quarterly reviews of biophysics*. 2008; 41:41–101. [PubMed: 18755053]
4. Dong KC, Berger JM. Structural basis for gate-DNA recognition and bending by type IIA topoisomerases. *Nature*. 2007; 450:1201–1205. [PubMed: 18097402]
5. Bax BD, Chan PF, Eggleston DS, Fosberry A, Gentry DR, Gorrec F, et al. Type IIA topoisomerase inhibition by a new class of antibacterial agents. *Nature*. 2010; 466:935–940. [PubMed: 20686482]
6. Corbett KD, Berger JM. Structural dissection of ATP turnover in the prototypical GHL ATPase TopoVI. *Structure*. 2005; 13:873–882. [PubMed: 15939019]
7. Stanger FV, Dehio C, Schirmer T. Structure of the N-terminal Gyrase B fragment in complex with ADPPi reveals rigid-body motion induced by ATP hydrolysis. *PloS one*. 2014; 9:e107289. [PubMed: 25202966]
8. Brown PO, Cozzarelli NR. A sign inversion mechanism for enzymatic supercoiling of DNA. *Science*. 1979; 206:1081–1083. [PubMed: 227059]
9. Corbett KD, Schoeffler AJ, Thomsen ND, Berger JM. The structural basis for substrate specificity in DNA topoisomerase IV. *J Mol Biol*. 2005; 351:545–561. [PubMed: 16023670]
10. Liu LF, Wang JC. *Micrococcus luteus* DNA gyrase: active components and a model for its supercoiling of DNA. *Proc Natl Acad Sci U S A*. 1978; 75:2098–2102. [PubMed: 276855]
11. Liu LF, Wang JC. DNA-DNA gyrase complex: the wrapping of the DNA duplex outside the enzyme. *Cell*. 1978; 15:979–984. [PubMed: 153201]
12. Orphanides G, Maxwell A. Evidence for a conformational change in the DNA gyrase-DNA complex from hydroxyl radical footprinting. *Nucleic acids research*. 1994; 22:1567–1575. [PubMed: 8202356]
13. Morrison A, Cozzarelli NR. Contacts between DNA gyrase and its binding site on DNA: features of symmetry and asymmetry revealed by protection from nucleases. *Proc Natl Acad Sci U S A*. 1981; 78:1416–1420. [PubMed: 6262797]
14. Kampranis SC, Bates AD, Maxwell A. A model for the mechanism of strand passage by DNA gyrase. *Proc Natl Acad Sci U S A*. 1999; 96:8414–8419. [PubMed: 10411889]
15. Reece RJ, Maxwell A. The C-terminal domain of the *Escherichia coli* DNA gyrase A subunit is a DNA-binding protein. *Nucleic acids research*. 1991; 19:1399–1405. [PubMed: 1851291]
16. Kampranis SC, Maxwell A. Conversion of DNA gyrase into a conventional type II topoisomerase. *Proc Natl Acad Sci U S A*. 1996; 93:14416–14421. [PubMed: 8962066]
17. Corbett KD, Shultzaberger RK, Berger JM. The C-terminal domain of DNA gyrase A adopts a DNA-bending beta-pinwheel fold. *Proc Natl Acad Sci U S A*. 2004; 101:7293–7298. [PubMed: 15123801]
18. Ruthenburg AJ, Graybosch DM, Huetsch JC, Verdine GL. A superhelical spiral in the *Escherichia coli* DNA gyrase A C-terminal domain imparts unidirectional supercoiling bias. *J Biol Chem*. 2005; 280:26177–26184. [PubMed: 15897198]
19. Costenaro L, Grossmann JG, Ebel C, Maxwell A. Small-angle X-ray scattering reveals the solution structure of the full-length DNA gyrase A subunit. *Structure*. 2005; 13:287–296. [PubMed: 15698572]
20. Baker NM, Weigand S, Maar-Mathias S, Mondragon A. Solution structures of DNA-bound gyrase. *Nucleic acids research*. 2011; 39:755–766. [PubMed: 20870749]

21. Papillon J, Menetret JF, Batisse C, Helye R, Schultz P, Potier N, et al. Structural insight into negative DNA supercoiling by DNA gyrase, a bacterial type 2A DNA topoisomerase. *Nucleic acids research*. 2013; 41:7815–7827. [PubMed: 23804759]

22. Schmidt BH, Osheroff N, Berger JM. Structure of a topoisomerase II-DNA-nucleotide complex reveals a new control mechanism for ATPase activity. *Nat Struct Mol Biol*. 2012; 19:1147–1154. [PubMed: 23022727]

23. Bryant Z, Oberstrass FC, Basu A. Recent developments in single-molecule DNA mechanics. *Current opinion in structural biology*. 2012; 22:304–312. [PubMed: 22658779]

24. Lionnet T, Allemand JF, Revyakin A, Strick TR, Saleh OA, Bensimon D, et al. Single-molecule studies using magnetic traps. *Cold Spring Harbor protocols*. 2012; 2012:34–49. [PubMed: 22194259]

25. Gubaev A, Dagmar K. Potassium ions are required for nucleotide-induced closure of gyrase N-gate. *J Biol Chem*. 2012; 287:10916–10921. [PubMed: 22343632]

26. Gubaev A, Hilbert M, Klostermeier D. The DNA-gate of *Bacillus subtilis* gyrase is predominantly in the closed conformation during the DNA supercoiling reaction. *Proc Natl Acad Sci U S A*. 2009; 106:13278–13283. [PubMed: 19666507]

27. Gubaev A, Klostermeier D. DNA-induced narrowing of the gyrase N-gate coordinates T-segment capture and strand passage. *Proc Natl Acad Sci U S A*. 2011; 108:14085–14090. [PubMed: 21817063]

28. Gubaev A, Klostermeier D. The mechanism of negative DNA supercoiling: a cascade of DNA-induced conformational changes prepares gyrase for strand passage. *DNA repair*. 2014; 16:23–34. [PubMed: 24674625]

29. Lanz MA, Farhat M, Klostermeier D. The acidic C-terminal tail of the GyrA subunit moderates the DNA supercoiling activity of *Bacillus subtilis* gyrase. *J Biol Chem*. 2014; 289:12275–12285. [PubMed: 24563461]

30. Lanz MA, Klostermeier D. Guiding strand passage: DNA-induced movement of the gyrase C-terminal domains defines an early step in the supercoiling cycle. *Guiding strand passage: DNA-induced movement of the gyrase C-terminal domains defines an early step in the supercoiling cycle*. 2011

31. Lanz MA, Klostermeier D. The GyrA-box determines the geometry of DNA bound to gyrase and couples DNA binding to the nucleotide cycle. *Nucleic Acids Research*. 2012; 40:10893–10903. [PubMed: 22977179]

32. Deniz AA, Laurence TA, Dahan M, Chemla DS, Schultz PG, Weiss S. Ratiometric single-molecule studies of freely diffusing biomolecules. *Annual review of physical chemistry*. 2001; 52:233–253.

33. Roy R, Hohng S, Ha T. A practical guide to single-molecule FRET. *Nature methods*. 2008; 5:507–516. [PubMed: 18511918]

34. Papillon J, Menetret JF, Batisse C, Helye R, Schultz P, Potier N, et al. Structural insight into negative DNA supercoiling by DNA gyrase, a bacterial type 2A DNA topoisomerase. *Nucleic acids research*. 2013

35. Gore J, Bryant Z, Stone MD, Nollmann M, Cozzarelli NR, Bustamante C. Mechanochemical analysis of DNA gyrase using rotor bead tracking. *Nature*. 2006; 439:100–104. [PubMed: 16397501]

36. Basu A, Schoeffler AJ, Berger JM, Bryant Z. ATP binding controls distinct structural transitions of *Escherichia coli* DNA gyrase in complex with DNA. *Nat Struct Mol Biol*. 2012; 19:538–546. S1. [PubMed: 22484318]

37. Lebel P, Basu A, Oberstrass FC, Tretter EM, Bryant Z. Gold rotor bead tracking for high-speed measurements of DNA twist, torque and extension. *Nat Methods*. 2014

38. Comstock MJ, Ha T, Chemla YR. Ultrahigh-resolution optical trap with single-fluorophore sensitivity. *Nature methods*. 2011; 8:335–340. [PubMed: 21336286]

39. Long X, Parks JW, Bagshaw CR, Stone MD. Mechanical unfolding of human telomere G-quadruplex DNA probed by integrated fluorescence and magnetic tweezers spectroscopy. *Nucleic acids research*. 2013; 41:2746–2755. [PubMed: 23303789]

40. Graves ET, Duboc C, Fan J, Stransky F, Leroux-Coyau M, Strick TR. A dynamic DNA-repair complex observed by correlative single-molecule nanomanipulation and fluorescence. *Nature structural & molecular biology*. 2015; 22:452–457.

41. Bates AD, O'Dea MH, Gellert M. Energy coupling in *Escherichia coli* DNA gyrase: the relationship between nucleotide binding, strand passage, and DNA supercoiling. *Biochemistry*. 1996; 35:1408–1416. [PubMed: 8634270]

42. Tretter EM, Berger JM. Mechanisms for defining supercoiling set point of DNA gyrase orthologs: I. A nonconserved acidic C-terminal tail modulates *Escherichia coli* gyrase activity. *J Biol Chem*. 2012; 287:18636–18644. [PubMed: 22457353]

43. Baird CL, Harkins TT, Morris SK, Lindsley JE. Topoisomerase II drives DNA transport by hydrolyzing one ATP. *Proc Natl Acad Sci U S A*. 1999; 96:13685–13690. [PubMed: 10570133]

44. Sugino A, Higgins NP, Brown PO, Peebles CL, Cozzarelli NR. Energy coupling in DNA gyrase and the mechanism of action of novobiocin. *Proc Natl Acad Sci U S A*. 1978; 75:4838–4842. [PubMed: 368801]

45. Bustamante C, Chemla YR, Forde NR, Izhaky D. Mechanical processes in biochemistry. *Annual review of biochemistry*. 2004; 73:705–748.

46. Nollmann M, Stone MD, Bryant Z, Gore J, Crisponi NJ, Hong SC, et al. Multiple modes of *Escherichia coli* DNA gyrase activity revealed by force and torque. *Nat Struct Mol Biol*. 2007; 14:264–271. [PubMed: 17334374]

47. Fernandez-Sierra M, Shao Q, Fountain C, Finzi L, Dunlap DE. *coli* Gyrase Fails to Negatively Supercoil Diaminopurine-Substituted DNA. *Journal of molecular biology*. 2015; 427:2305–2318. [PubMed: 25902201]

48. Peter BJ, Arsuaga J, Breier AM, Khodursky AB, Brown PO, Cozzarelli NR. Genomic transcriptional response to loss of chromosomal supercoiling in *Escherichia coli*. *Genome Biol*. 2004; 5:R87. [PubMed: 15535863]

49. van Workum M, van Dooren SJ, Oldenburg N, Molenaar D, Jensen PR, Snoep JL, et al. DNA supercoiling depends on the phosphorylation potential in *Escherichia coli*. *Mol Microbiol*. 1996; 20:351–360. [PubMed: 873233]

50. Cheung KJ, Badarinarayana V, Selinger DW, Janse D, Church GM. A microarray-based antibiotic screen identifies a regulatory role for supercoiling in the osmotic stress response of *Escherichia coli*. *Genome research*. 2003; 13:206–215. [PubMed: 12566398]

51. Vijayan V, Zuzow R, O'Shea EK. Oscillations in supercoiling drive circadian gene expression in cyanobacteria. *Proc Natl Acad Sci U S A*. 2009; 106:22564–22568. [PubMed: 20018699]

52. Liu LF, Wang JC. Supercoiling of the DNA template during transcription. *Proc Natl Acad Sci U S A*. 1987; 84:7024–7027. [PubMed: 2823250]

53. Postow L, Hardy CD, Arsuaga J, Cozzarelli NR. Topological domain structure of the *Escherichia coli* chromosome. *Genes Dev*. 2004; 18:1766–1779. [PubMed: 15256503]

54. Chong S, Chen C, Ge H, Xie XS. Mechanism of transcriptional bursting in bacteria. *Cell*. 2014; 158:314–326. [PubMed: 25036631]

55. Taniguchi Y, Choi PJ, Li GW, Chen H, Babu M, Hearn J, et al. Quantifying *E. coli* proteome and transcriptome with single-molecule sensitivity in single cells. *Science*. 2010; 329:533–538. [PubMed: 20671182]

56. Howard J. Mechanical signaling in networks of motor and cytoskeletal proteins. *Annu Rev Biophys*. 2009; 38:217–234. [PubMed: 19416067]

57. Tretter EM, Berger JM. Mechanisms for defining supercoiling set point of DNA gyrase orthologs: II. The shape of the Gyra subunit C-terminal domain (CTD) is not a sole determinant for controlling supercoiling efficiency. *J Biol Chem*. 2012; 287:18645–18654. [PubMed: 22457352]

58. Rovinskyi N, Agbleke AA, Chesnokova O, Pang Z, Higgins NP. Rates of gyrase supercoiling and transcription elongation control supercoil density in a bacterial chromosome. *PLoS genetics*. 2012; 8:e1002845. [PubMed: 22916023]

59. Pato ML, Howe MM, Higgins NP. A DNA gyrase-binding site at the center of the bacteriophage Mu genome is required for efficient replicative transposition. *Proc Natl Acad Sci U S A*. 1990; 87:8716–8720. [PubMed: 2174162]

60. Oram M, Howells AJ, Maxwell A, Pato ML. A biochemical analysis of the interaction of DNA gyrase with the bacteriophage Mu, pSC101 and pBR322 strong gyrase sites: the role of DNA sequence in modulating gyrase supercoiling and biological activity. *Molecular microbiology*. 2003; 50:333–347. [PubMed: 14507384]

61. Yang Y, Ames GF. DNA gyrase binds to the family of prokaryotic repetitive extragenic palindromic sequences. *Proc Natl Acad Sci U S A*. 1988; 85:8850–8854. [PubMed: 2848243]

62. Espeli O, Boccard F. In vivo cleavage of *Escherichia coli* BIME-2 repeats by DNA gyrase: genetic characterization of the target and identification of the cut site. *Molecular microbiology*. 1997; 26:767–777. [PubMed: 9427406]

63. Liu LF, Wang JC. Supercoiling of the DNA template during transcription. *Proc Natl Acad Sci U S A*. 1987; 84:7024–7027. [PubMed: 2823250]

64. Ma J, Bai L, Wang MD. Transcription under torsion. *Science*. 2013; 340:1580–1583. [PubMed: 23812716]

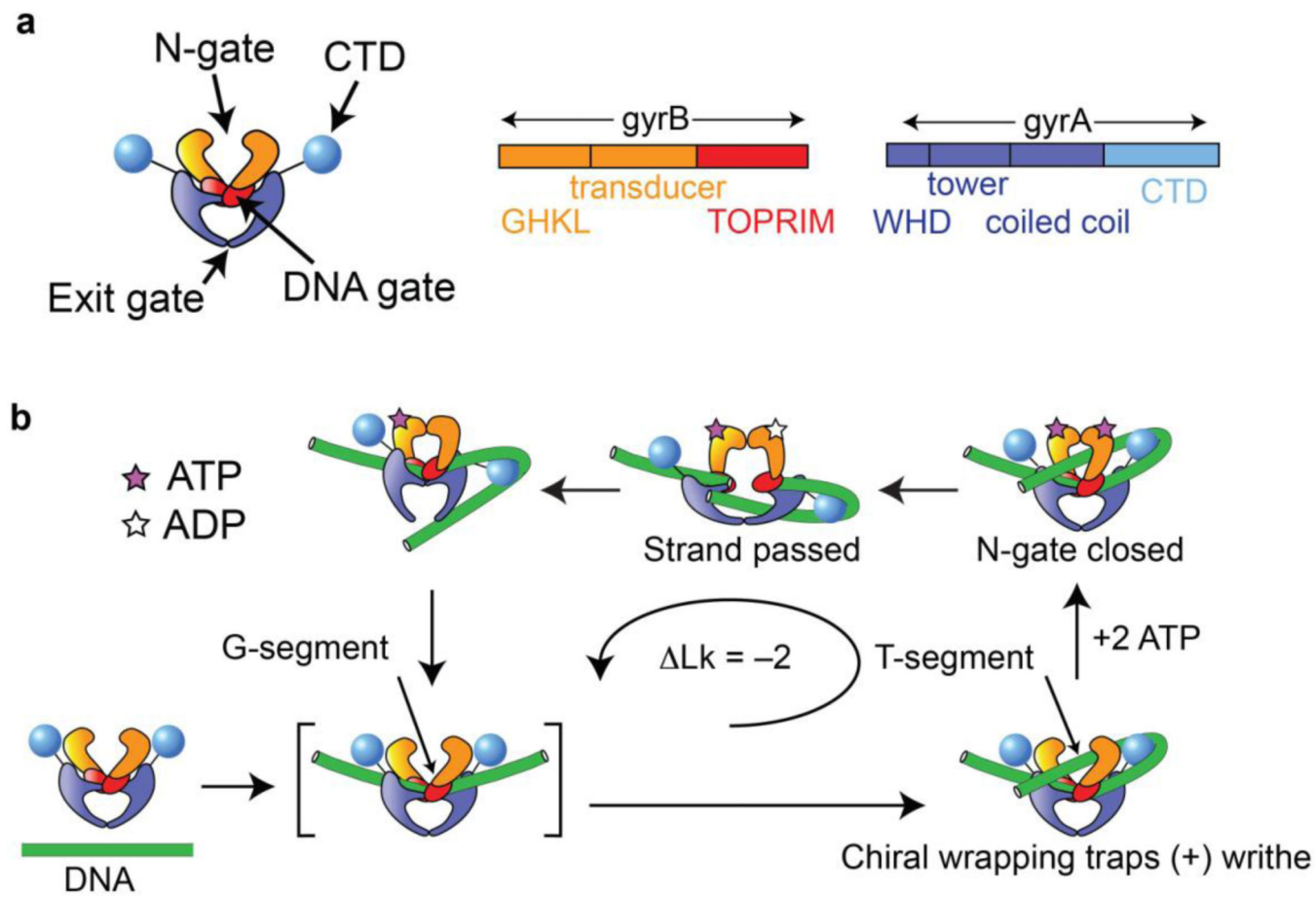
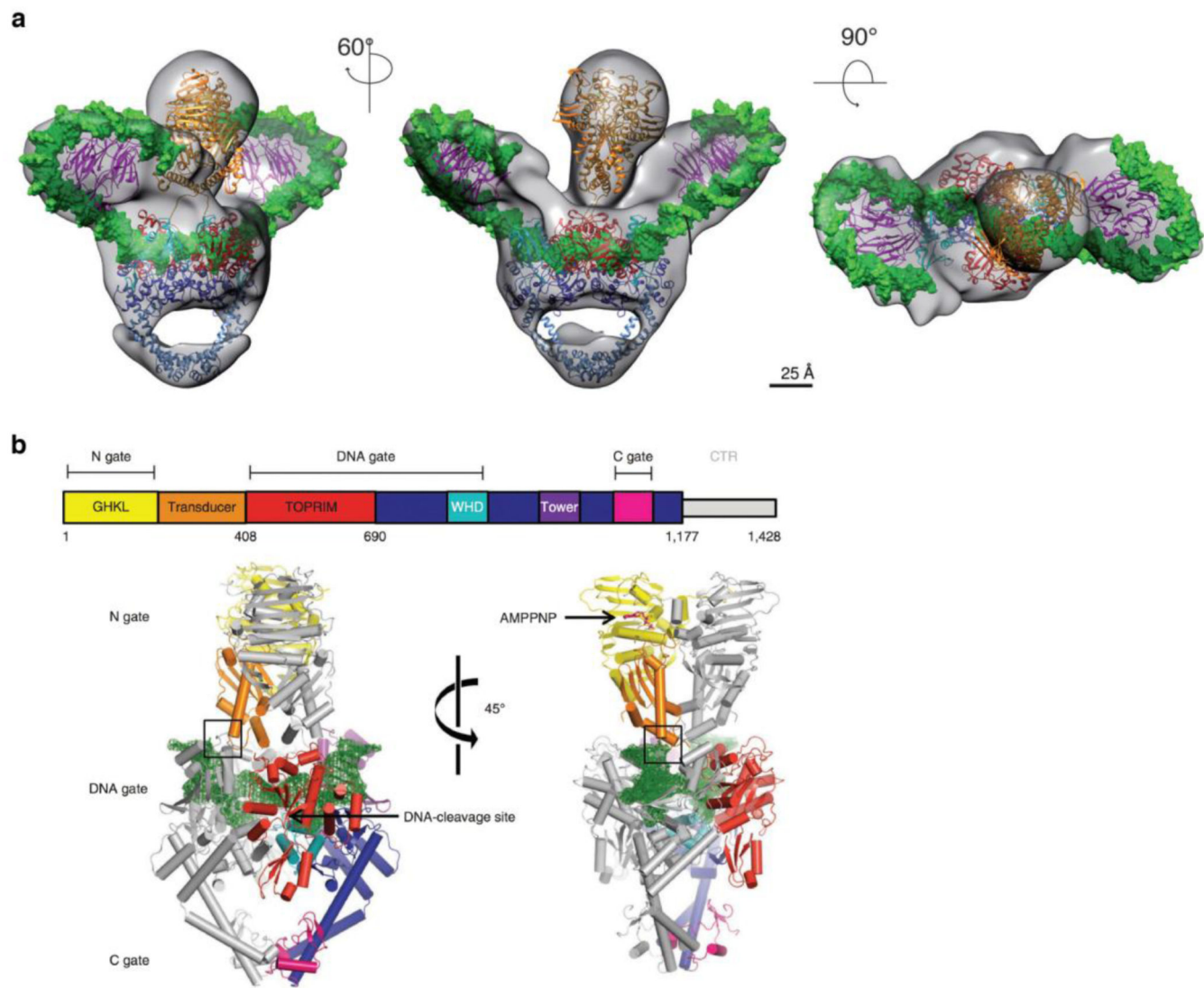
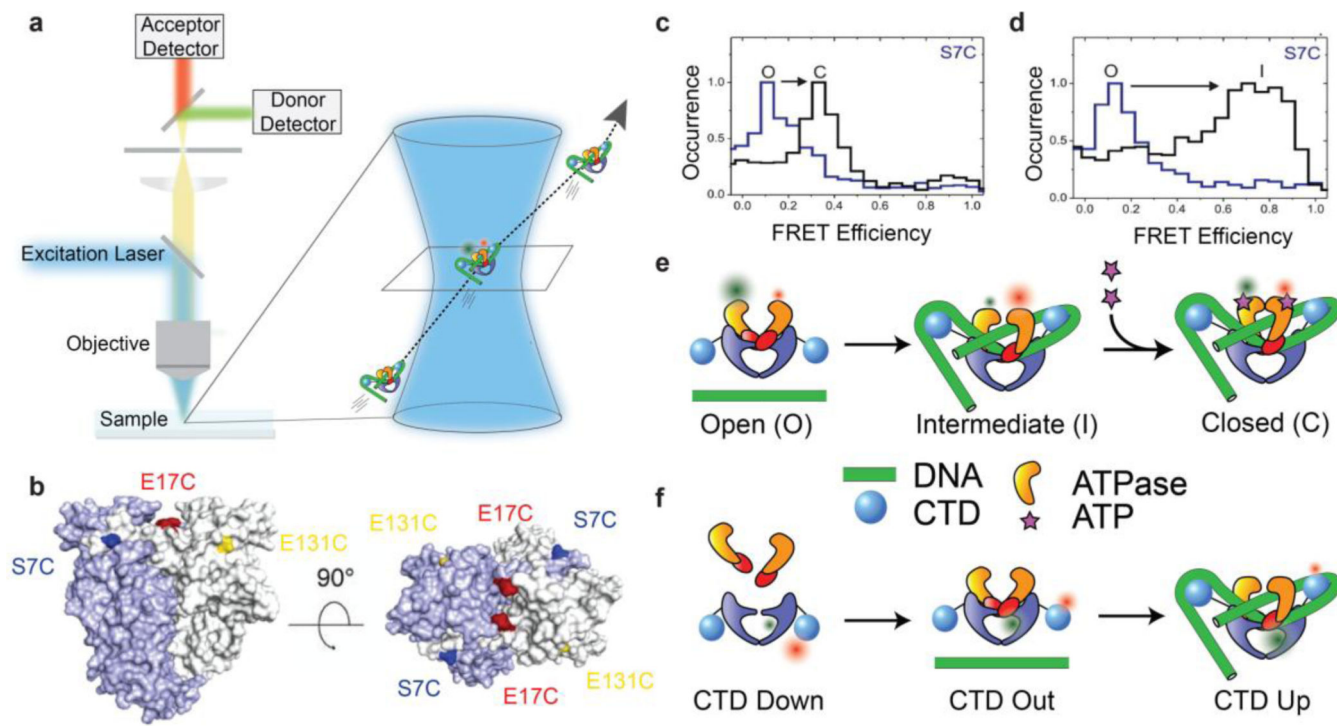


Figure 1.
 Composition and basic mechanism of DNA gyrase. (a) Cartoon showing domain organization. Gyrase is an A_2B_2 heterotetramer. Interfaces between the subunits form three gates that can be opened and closed. (b) Outline of the enzymatic cycle. The G-segment binds to the central DNA gate. Chiral wrapping presents a proximal T-segment within the N-gate cavity. ATP binding induces N-gate closure, followed by passage of the T-segment through the transiently cleaved G-segment and expulsion through the C-gate. One round of strand passage leads to the introduction of two negative supercoils.

**Figure 2.**

Recent structures illuminate the architectures of gyrase and related type II topoisomerases. (a) 23 Å CryoEM map of the *T. thermophilus* gyrase holoenzyme in complex with 155 bp DNA, ciprofloxacin, and AMPPNP (reproduced from [21]). The domain architecture can be seen together with density attributable to DNA wrapped around the CTDs. Crystal structures of protein components and modeled DNA duplex (green) have been fit to the density. The closed N-gate is shown in a domain-swapped configuration first observed in (b) a crystal structure (reproduced from [22]) of the related enzyme *S. cerevisiae* topo II in complex with G-segment DNA (green) and AMPPNP. The DNA-gate and the C-gate are also seen in closed configurations in these structures.

**Figure 3.**

Single-molecule FRET reveals DNA and nucleotide dependent conformations of *B. subtilis* DNA gyrase. (a) Schematic of confocal smFRET microscopy (not to scale). Labeled complexes diffusing through the femtoliter confocal volume produce brief bursts of fluorescence that are collected on donor and acceptor channels to measure distributions of FRET efficiencies. (b) FRET labeling positions used for probing N-gate conformations (reproduced from [27]). (c-d) N-gate FRET histograms for gyrase using the S7C labeling position (reproduced from [27]), showing three N-gate conformations labeled O (open), C (closed), and I (intermediate/narrowed). For this labeling position, FRET is lower in the closed state than the intermediate state, explained by the N-terminal location of S7C in the intertwined dimerized ATPase domains. (c) No nucleotide (blue) vs ADPNP (black), in the absence of DNA. (d) No DNA (black) vs relaxed plasmid DNA (blue), in the absence of nucleotide. (e) Cartoons of N-gate conformations probed by FRET. (f) Cartoons of CTD positions based on smFRET measurements between the gyrA CTD and the core enzyme [30]. CTDs are positioned toward the exit gate in the gyrA dimer alone, move out slightly when gyrB is bound, and swing up when the enzyme is complexed with DNA.

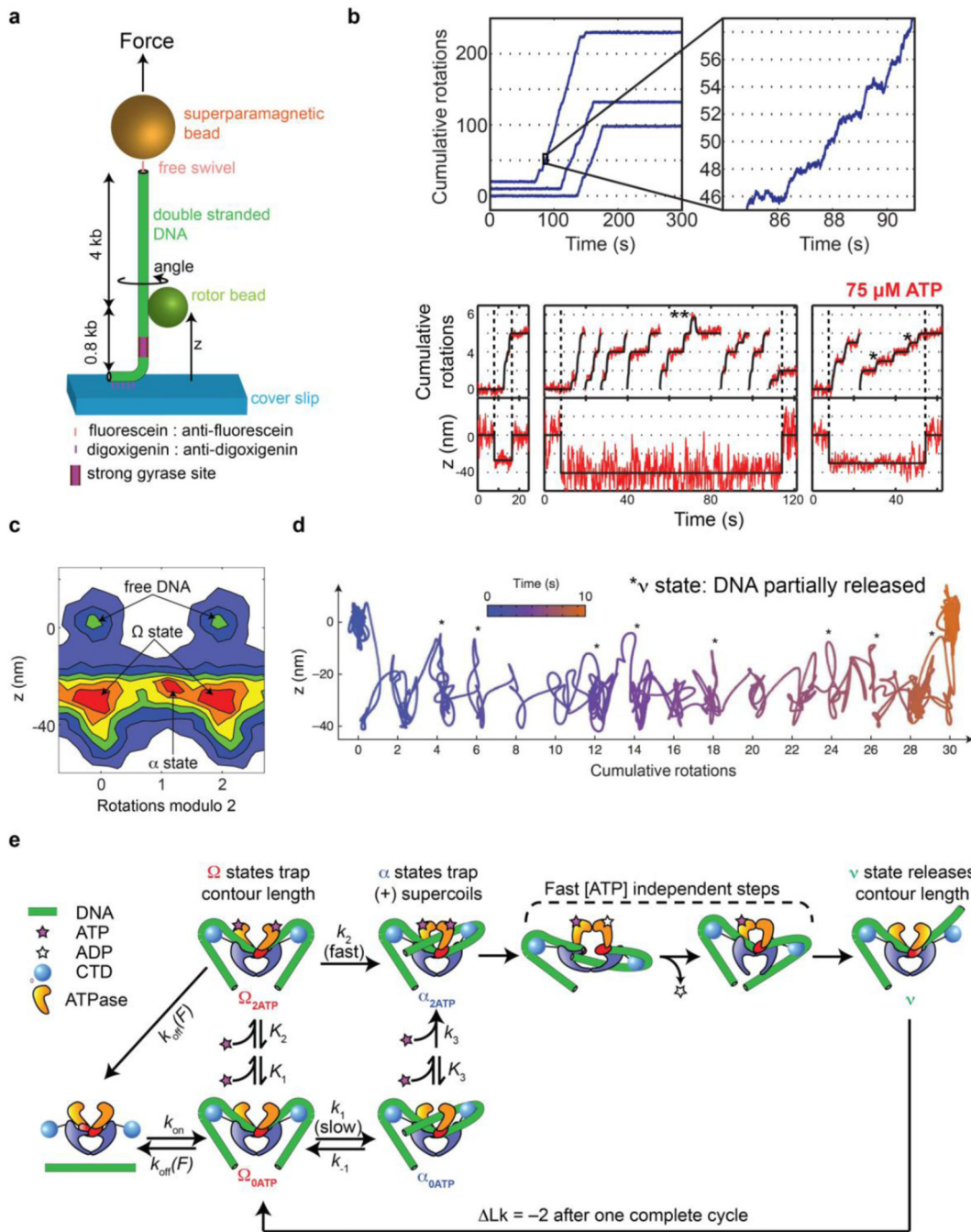
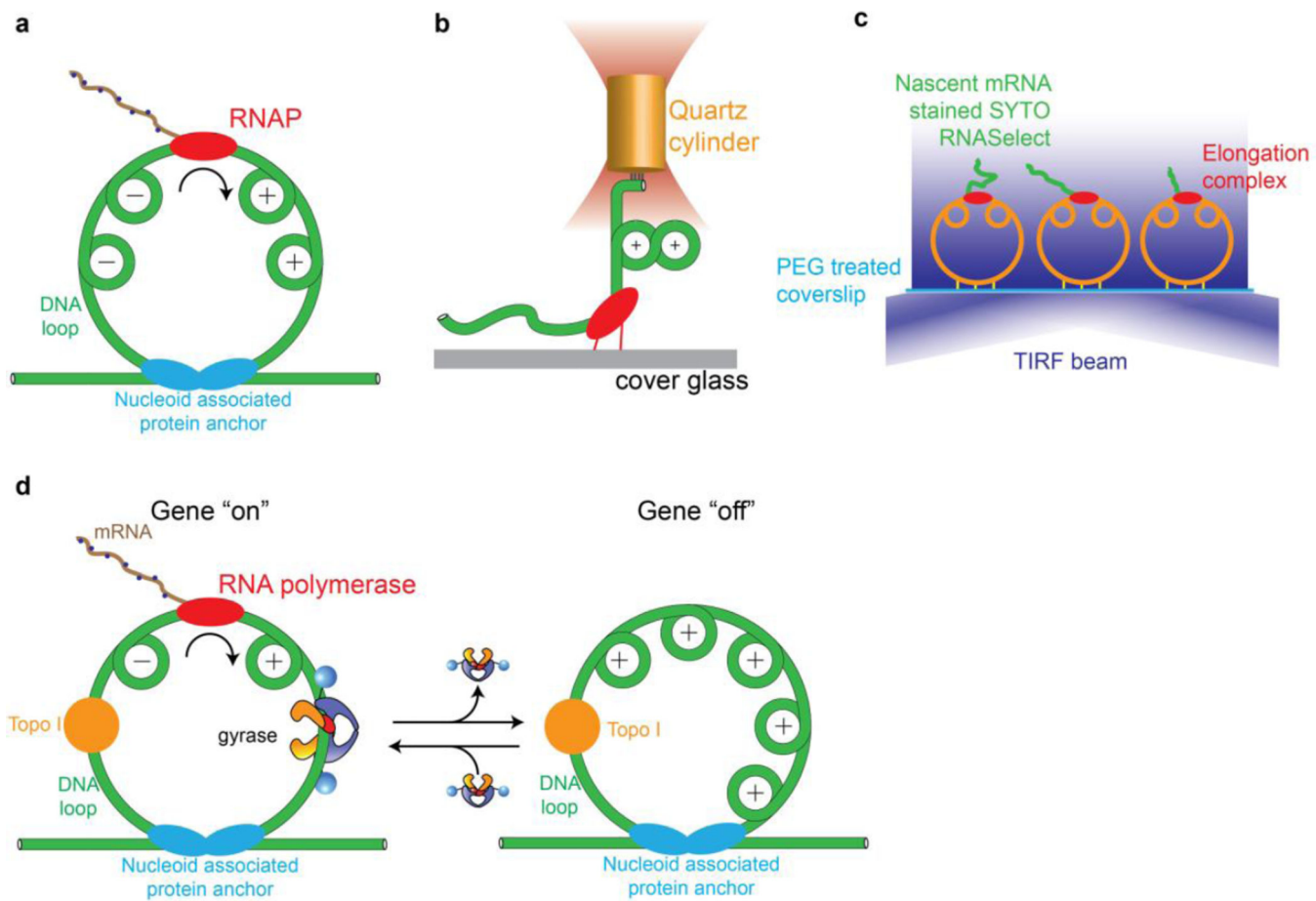


Figure 4.
 Rotor bead tracking reveals new conformations and ATP-dependent dynamics of *E. coli* DNA gyrase. (a) The rotor bead tracking (RBT) assay. DNA is stretched using a magnetic bead, and a submicron rotor bead is attached to the side of the molecule and tracked using fluorescence [35] [36] or evanescent scattering [37] videomicroscopy to measure changes in DNA angle and extension (z) in real time. (b) RBT traces (reproduced from [36]) in the presence of DNA gyrase under in 1 mM ATP (above) or 75 μ M ATP (below). Individual gyrase encounters lead to bursts of stepwise rotation, corresponding to processive negative

supercoiling. [ATP]-dependent dwells are seen at the even rotation mark and also at an intermediate angle (*) corresponding to a chirally wrapped intermediate. (c) 2D histogram (reproduced from [36]) of paired (angle,z) values during gyrase activity in presence of 75 μ M ATP, showing distinct conformational states visited by the enzyme. Angles are shown modulo 2 rotations. The Ω state is significantly contracted in z but lies at the ~0 rotation mark, which is explained by sequestering DNA contour without trapping writhe. The α state can also be seen at the ~1 rotation mark, corresponding to trapping (+) writhe prior to strand passage. (d) High-resolution dynamics of gyrase at 1 mM ATP using gold rotor bead tracking (reproduced from [37]). A single processive burst is shown in the (angle, z) plane. Major dwells are interrupted by brief excursions to a state (*) that releases significant contour length. (e) Branched kinetic model for structural transitions and ATP coupling in DNA gyrase [36, 37]. The kinetics of processive supercoiling are dominated by the transition from Ω to α , which can occur slowly and reversibly in the absence of ATP or quickly when 2 ATP are bound. Subsequent strand passage also requires the presence of 2 ATP. DNA is partially released after strand passage and recaptured to begin a new round of supercoiling.

**Figure 5.**

Mechanical interplay of gyrase, transcription, and DNA supercoiling investigated using single-molecule methods. (a) Helical tracking of the advancing transcription complex leads to twin supercoiling domains in a constrained DNA duplex [54, 63]. (b) An optical torque wrench assay [64] showed that RNA polymerase stalls due to positive supercoils that accumulate ahead of the enzyme, with a measured stall torque of ~ 10 pN nm. (c) Single-molecule assay for transcription on tethered constrained circular templates [54]. Fluorescence accumulates during transcription due to an RNA-binding dye. Dynamics can be investigated in the presence of gyrase and/or topoisomerase I. (d) Model for transcriptional bursting based on single-molecule measurements [54]. Topoisomerase I constitutively relieves (-) supercoils behind the transcription complex, leading to the accumulation of (+) supercoils in a constrained chromosomal loop. When gyrase is bound, (+) supercoils are relaxed and transcription can proceed. When gyrase dissociates, accumulated (+) supercoils inhibit transcription, intermittently shutting off gene expression.